Design of the Battery Management System of $LiFePO_4$ Batteries for Electric Off-Road Vehicles

F. Baronti, G. Fantechi, R. Roncella, R. Saletti
Dip. Ingegneria dell'Informazione, University of Pisa
Via Caruso 16, 56122 Pisa, Italy

G. Pede, F. Vellucci
ENEA - Centro Ricerche Casaccia
Via Anguillarese 301, 00123 S. Maria di Galeria (RM), Italy

***Abstract*—This paper describes the design of a modular battery management system for electric off-road vehicles, where lithium-ion batteries are expected to be widely used. A massive electrification of off-road vehicles can be enabled by the availability of a standard battery module, provided with an effective management unit. The design and some preliminary experimental results of the module management unit are discussed in this paper. The unit contains a high current active equalizer that enables the dynamic charge equalization among cells and maximizes the usable capacity of the battery.**

***Keywords*—Battery Management System, Active balancing, Electric Off-Road Vehicles, Lithium-ion battery technology**

I. Introduction

Off-road vehicles used in many commercial and industrial activities are a large portion of means of transportation. These vehicles include mobile work machines for various applications, such as building sites, earth moving, street cleaning, as well as agriculture, horticulture, greenhouse, and gardening. An internal combustion engine commonly powers off-road vehicles. The replacement or the combination of this engine with an electric motor might be a remarkable step toward energy sustainability by reducing CO_2 emissions and by improving energy utilization efficiency [1], [2].

A recent study on the Italian market for mobile work machines gives a good idea of the relevance of these kinds of vehicles and the impact of their electrification [2]. Figure 1 shows the forecasted sales of electric off-road vehicles, grouped by function and expressed in terms of onboard battery energy. These numbers have been obtained by firstly estimating the sales volumes of the various kinds of mobile work machines in 2020. Then, the appropriate sizing of the battery, in terms of stored energy and power, has been evaluated for each category of work machine. Finally, the penetration of the electric models has been estimated as 10 % of the market. To gather the relevance of the potential battery market for electric mobile work machines, let us express it in terms of equivalent electric cars. Assuming 25 kWh as the energy capacity of an electric car battery, the estimated market for electric mobile work machines in Italy by 2020 is equivalent to 20 k electric cars. Considering 2 M cars as the overall Italian car market in 2020 and that optimistically 4 % of the new cars is electric, we end up with the surprising conclusion that the battery market for electric mobile work machines will be 25 % of the batteries used in electric cars.

The above sketched scenario is very promising for the electrification of off-road vehicles. The success of this transformation is deeply connected to the availability of an energy storage system that addresses the specific constraints of each off-road vehicle category, which has its own requirements in terms of battery voltage and capacity. It is thus important to identify a *standard* battery module, which can be used to build up the battery for each type of machine by connecting in series or parallel the required number of standard modules. This standardization effort is very significant, as it might help in reducing the overall battery cost, which is the major limiting factor for the electric transformation of these kinds of vehicles.

The standard battery module consists of 4 series-connected lithium-ion cells ($LiFePO_4$ units), according to the study in [2]. Here, the focus is on the design of the relevant battery management system (BMS). The BMS is a fundamental component for an effective use of lithium-ion batteries. Lithium-ion battery technology provides several advantages in terms of higher energy and power densities, higher charge/discharge efficiency, and longer lifetime as compared to the more traditional valve-regulated lead-acid or nickel-metal-hydride technologies. However, lithium-ion cells are very fragile and sensitive to overcharge, deep discharge, and over temperature. These conditions might shorten the battery lifetime (accelerating capacity fading and internal resistance degradation mechanisms due to battery aging), but even cause destructive damages to the battery itself. Thus, the major function of a BMS is to protect the battery against hazardous

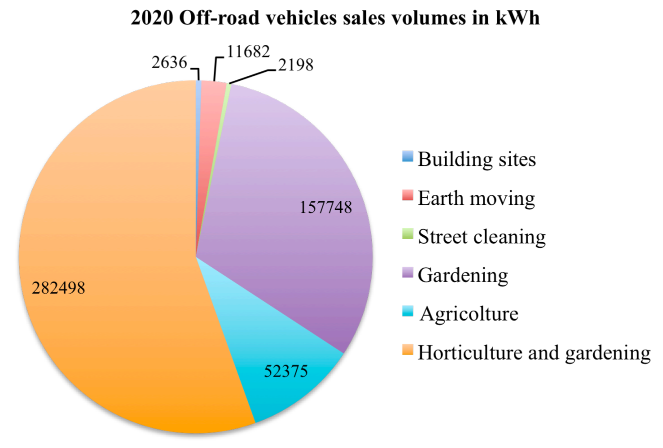

Figure 1. Estimated sales volumes for electric mobile work machines, expressed in terms of capacity of the onboard battery [2].

situations by monitoring the voltage and the temperature of the cells that build up the battery. Extending battery life is dramatically important because the battery cost represents a large percentage of the overall cost of a typical electric mobile work machine.

Furthermore, batteries consisting of series-connected cells tend to become unbalanced over time (a condition in which some cells store more energy than others). This is due to the variability of the cell parameters (mainly the self-discharge rate) and of the operating conditions (e.g. temperature gradient in the battery). The net consequence is a reduction of the usable battery capacity. In fact, when the least charged cell reaches the discharge cut-off voltage, the battery current has to be stopped to protect that cell, while there is still energy in the other cells. Unfortunately, unbalancing in a lithium-ion battery cannot be self-recovered as it can in more traditional technologies, which can tolerate a controlled overcharge of the more charged cells. On the contrary, recharging of a lithium-ion battery has to be stopped when the most charged cell reaches the upper voltage limit, causing the other cells not to be fully recharged. Thus, an appropriate circuit is needed to restore the balanced condition. The simplest technique consists of connecting a shunt resistor in parallel to the more charged cells (passive balancing). This way, the balanced condition is reached by dissipating the extra energy stored in the more charged cells. Active techniques, where charge equalization is obtained by transferring energy from more charged cells to lower charged ones [3], have been proposed to avoid wasting energy. Research focuses on improving efficiency, reducing implementation complexity and balancing time [3]–[7].

II. STANDARD BATTERY MODULE

The standard battery module consists of 4 series-connected $LiFePO_4$ cells, as described in [2]. The module nominal voltage is 12.8 V, whereas the discharge and charge cut-off voltages are 10 V and 15.4 V, respectively. This allows the standard module to be used in place of a conventional lead acid battery, commonly found in any vehicle for starting, lighting, and ignition [8]. A huge market with potential great benefits in terms of cost reduction is expected. The proposed standard module can be very effective in meeting the different battery voltage specifications found in the electrification of the various types of mobile work machines. For instance, a large portion of these vehicles is powered by a 48 V battery, which can be implemented by series-connecting 4 standard modules. The standard module can host three different cell capacities: 30 Ah, 60 Ah, and 100 Ah, in order to address the different requirements for the stored energy and battery runtime.

It is worth noting that the standard module contains a relatively small number of cells. Thus, the cost overhead related to module assembling and BMS, which do not scale with the number of cells, is more significant than in a coarser-grained partitioning of the battery pack. However, these costs are by far counterbalanced by the availability of a standard module fully compatible with a lead acid battery with the benefits of the lithium-ion battery technology. $LiFePO_4$ cells are more robust and cheaper than other lithium-ion cells, at the expense of a lower energy density. On the other hand, electric off-road vehicles have less stringent constraints on the battery

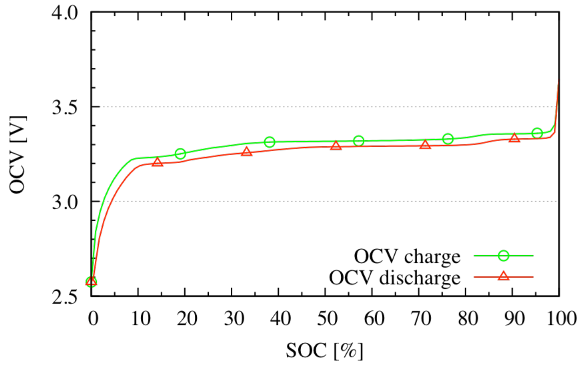

Figure 2. Open circuit voltage (OCV) versus State-of-charge (SOC) measured on a 60 Ah $LiFePO_4$ cell (manufactured by Hipower).

weight and volume compared to other electric vehicles. Therefore, $LiFePO_4$ battery technology has been selected for implementing the standard module. Figure 2 shows the relationship between open circuit voltage (OCV) and state of charge (SOC) measured on a 60 Ah $LiFePO_4$ (from Hipower), showing the flatness of the characteristics and the hysteresis effect between charge and discharge.

III. BMS DESIGN

A. *BMS architecture*

The effective partitioning and implementation of the BMS functions is crucial when a large number of series-connected cells are managed. We proposed to solve the problem by considering the battery as a hierarchical platform consisting of three layers: the elementary cell, the module (i.e. a subset of adjacent series-connected cells, usually assembled in a dedicated case) and the pack (a connection of modules) [9]. This perspective leads to a clear, general and easy to implement partitioning of the BMS functions [10]. In fact, fundamental monitoring tasks (cell voltage and temperature measurement), as well as passive balancing, lie on the lowest layer of the platform, i.e. the cell. Charge transfer between cells (to achieve active equalization) and thermal management belong to the intermediate layer, namely the module. Battery protection (by a main switch or contactor) and more advanced functions, such as state-of-charge (SOC) and state-of-health (SOH) estimation, are mapped in the uppermost layer of the platform. SOC is usually evaluated as the amount of charge stored in a cell as a percentage of the actual capacity value. The latter might differ from the nominal value due to variations in the manufacturing process and cell ageing (capacity fading effect). SOH expresses the ratio of the capacity value to the nominal one. The pack layer is also provided with interfaces to communicate with external systems, for example the vehicle management unit in an electric vehicle application or a personal computer for data acquisition and configuration of the BMS.

Given the above logic partitioning, which is independent of the battery size and organization, the fundamental issue is how to effectively map the logic layers of the platform into their hardware counterparts. This step instead depends on the actual composition of the battery and on the targeted application, as the latter determines the requirements in terms of safety levels and advanced function implementation. Although there are attractive implementations of the logic cell layer into a dedicated electronic board applied to each single cell of the battery [11], [12], these solutions are less effective when the module consists of a small number of cells, as in our standard module, which contains 4 cells. In addition, these solutions may hardly be compatible with the module assembling constraints that are determined by the application. Thus, the cell layer merges with the module layer in our BMS. This design choice is quite common and is confirmed by the availability of off-the-shelf components designed to measure the voltage of up to 12 cells, the temperature in one or two spots and to carry out passive balancing. Figure 3 shows the devised BMS architecture in the case of a battery consisting of 4 standard modules. The MMU (Module Management Unit) implements the module logic layer functions, such as active balancing and thermal management, but also the cell logic layer functions, such as monitoring the voltage and temperature of the 4 cells of the module.

The pack logic layer carries out functions such as SOC and SOH estimation and data logging, which can be implemented by software routines. Thus, there are various options for mapping this logic layer into hardware. A possible choice is to implement the high level BMS software functions as further tasks of the firmware running on the main control unit of the application, such as the vehicle management system. Although this solution is attractive as it does not require any additional piece of hardware, it is strongly dependent on the targeted application, particularly on the free computational resources available on the processor of the main control unit. As a consequence, this approach is not appropriate to achieve our goal of assembling the battery for a wide range of applications by using standard battery modules. On the other hand, the use of dedicated hardware (e.g. a centralized pack management unit, PMU) to map the logic pack layer, as proposed in many publications (e.g. [6], [13]–[15]), would be hardly affordable for many mobile work machines, where the battery requires a small number of standard modules.

We instead propose to distribute the pack logic layer functions to the MMUs as much as possible. For instance, advanced SOC and SOH algorithms based on a cell model ([16], [17]) can be executed at the module rather than at the pack level. Distributing high level functions on different processors instead of a single one (embedded in the PMU) also reduces the communication requirements between MMU and PMU and increases the system reliability. The remaining centralized functions can be mapped onto a particular MMU, which takes the role of master, whereas the other MMUs act as slaves. It is worth noting that the centralized functions, such as supervising and coordinating the behavior of the slave MMUs, measuring the battery current and controlling the main battery switch, are a very small portion of the overall functions of a MMU. The corresponding overhead is minimal so that a standard module can assume the role of master by only changing some firmware configuration parameters that enable the relevant centralized functions. In that case, the additional peripherals (for instance the current sensor (I) and the pack protection switch (PPS)) will be connected to specific I/O pins on the MMU acting as master, as shown in Figure 3. As an example that proves the power of this flexible design approach, let us mention that a battery for starting, lighting, and igniting

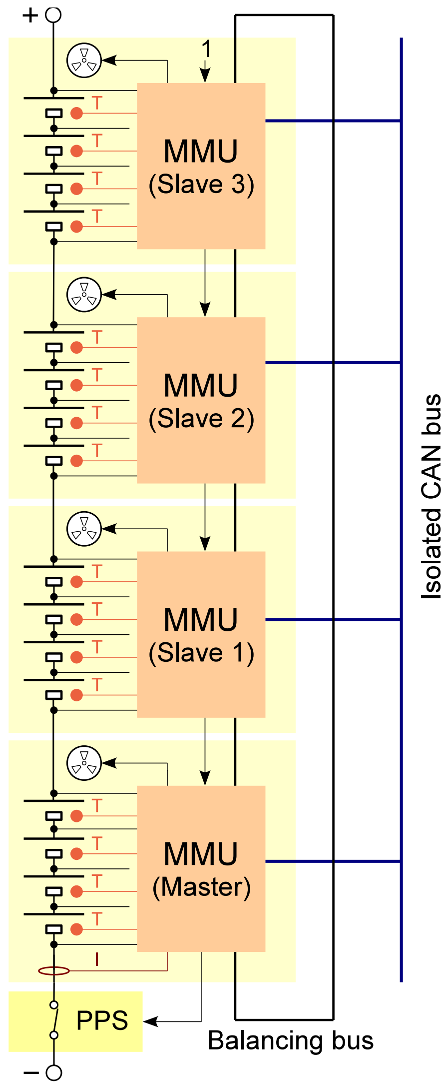

Figure 3. Architecture of the BMS sketched for a battery comprising of 4 standard modules. MMU is the module management unit and PPS is the pack protection switch.

an ordinary car can be obtained by just one standard module configured as a master.

Finally, it is interesting to note how the battery protection mechanism is distributed over all the MMUs. Each MMU asserts an internal logical variable (*Safe*) when all the voltages and temperatures of the 4 cells in the module are in their safe operating ranges. This variable is ANDed with the input enable signal produced by the preceding slave module in the chain to generate the output enable signal, as indicated in Figure 3. The output of the chain's last unit (the master MMU) is finally connected to the PPS, which breaks the battery current when an unsafe condition occurs in whichever module. The master MMU can also supervise the behavior of the slave MMUs and transmit the battery current value to them (if required by the SOC and SOH estimation algorithms implemented on each MMU) by means of an isolated CAN (Controller Area Network) bus. As most of the processing is performed at the module level, the communication requirements on this bus are low. Thus, the isolated CAN bus can also be used to connect

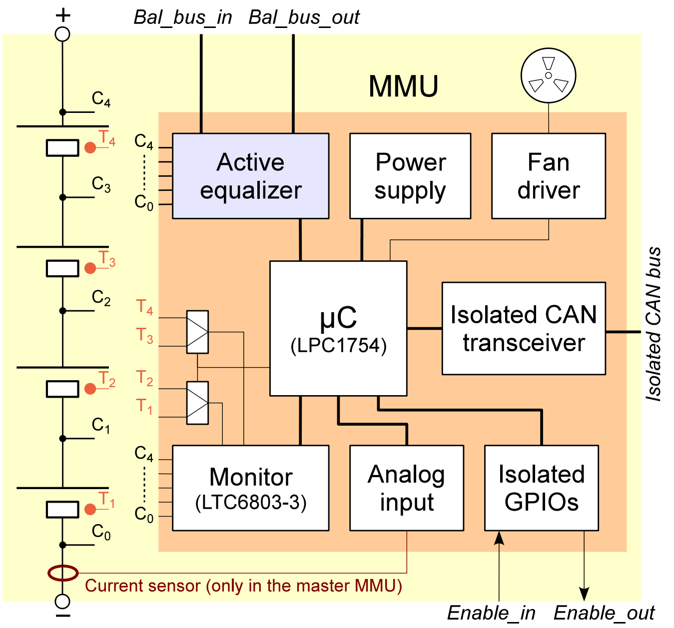

Figure 4. Block diagram of the module management unit (MMU).

the intelligent battery to other electronic units or to a PC for BMS configuration, diagnostics or data logging.

B. Module Management Unit design

As described above, the MMU is the hardware platform that implements the three logic layers in which the BMS functionalities are partitioned. In addition, the MMU hardware is always the same independently of the module role in the battery (master or slave), which will be defined by firmware configuration. Figure 4 shows the schematic block diagram of the MMU. The logic cell layer is implemented by a single chip (i.e. LTC6803-3 from Linear Technology), which measures the voltage (with 10 mV accuracy) and temperature of each module cell. As the LTC6803-3 provides only two channels for temperature measurements, the 4 NTC (Negative Temperature Coefficient) resistors are connected by means of two 2-way analog multiplexers controlled by the microcontroller. The NTCs are glued to each cell case in the spot where the highest temperature was measured by an infrared camera during high current tests. The Monitor chip is connected to the microcontroller via an SPI (Serial Peripheral Interface).

The microcontroller (i.e. LPC1754 from NXP, based on an ARM Cortex M3 processor with a 32 b data bus) is indeed the core of the MMU. It acquires the voltage and temperature of the cells and (if the MMU is configured as master) the battery current through a Hall Effect transducer (DHAB family from LEM) with 1 % typical accuracy. This sensor family provides two ratio-metric output channels with different measurement ranges. The sensor model to be placed in the master module is selected according to the capacity of the module cells (i.e. 30 Ah, 60 Ah, and 100 Ah) and the application specifications. The outputs of the sensor are read by the ADC embedded in the microcontroller. The sampling rate of the cell voltages and the battery current is 10 Hz, whereas cell temperatures are acquired at the lower rate of 1 Hz. The battery current value is transmitted by the MMU master on the isolated CAN bus. The microcontroller compares the voltage and temperature of the module cells, as well as the battery current, to configurable thresholds in order to carry out two of the major MMU tasks, i.e. battery protection and thermal management. In fact, as soon as one cell exceeds its safe operating range, the MMU enters into an error state in which the local *enable* of the PPS is disabled. This signal is ANDed with the *Enable_in* signal to generate the MMU output *Enable_out*. The Fan Driver block activates the module fan when one of the cell temperatures exceed a given threshold.

The MMU is powered by the module cells so that its power consumption is critical, as it might dramatically worsen the self-discharge rate of the battery. Thus, the microcontroller disables the power supply of certain blocks, when they are not needed, and enter low-power operating modes to implement the necessary power saving policy. Finally, the active equalizer is an innovative part of this design as it is capable of equalizing the energy stored in the 4 cells of the module, as well as to cooperate with the active equalizer of the two adjacent MMUs (through the *Bal_bus_in* and *Bal_bus_out* power buses) to balance the charge among modules also. This circuit will be described more in detail in the following sub-section.

C. Active balancing

The ultimate goal of an active balancing technique is to maintain an even distribution of charge among series-connected cells of a battery over time, with ideally no energy losses for the equalization process. This makes it possible to exploit all the energy stored in the battery (i.e. to maximize the usable capacity of the battery). In contrast with passive balancing, a non dissipative element, such as a capacitor or an inductor, is used as tank to transfer energy between the cells of the battery in every active balancing circuit. The circuits presented in the literature so far can achieve very high energy transfer, but usually provide very low balancing currents (around a few hundreds of milliamperes), limiting the amount of charge that can be transferred in a given time. Increasing the balancing current requires the use of bulky passive components (capacitors, inductors or transformers), which is not affordable in many of the proposed techniques, and also negatively affects the efficiency, as conduction losses increase.

In addition, these circuits aim at counterbalancing differences in the cell self-discharge rates, which produce an appreciable imbalance in the SOC of the battery cells in the range of months (or even weeks). Thus, low balancing currents can be used to periodically equalize the SOC of the cells. This phase is usually carried out at the end of a battery recharge to bring all the cells at 100 % SOC. However, this does not necessarily mean that every cell stores the same amount of charge or energy. This is due to mismatches in the capacity values caused by variations in the manufacturing process or in the operating conditions (particularly the temperature) that significantly affects the speed of the capacity fading effect. Then, even if all the cells are initially fully charged (100 % SOC), the cell with the lowest capacity will reach the discharge cut-off voltage before the others, causing the interruption of the battery current while there is still energy in the battery. The net consequence is that the usable capacity of the battery is determined by the cell with the minimum capacity value.

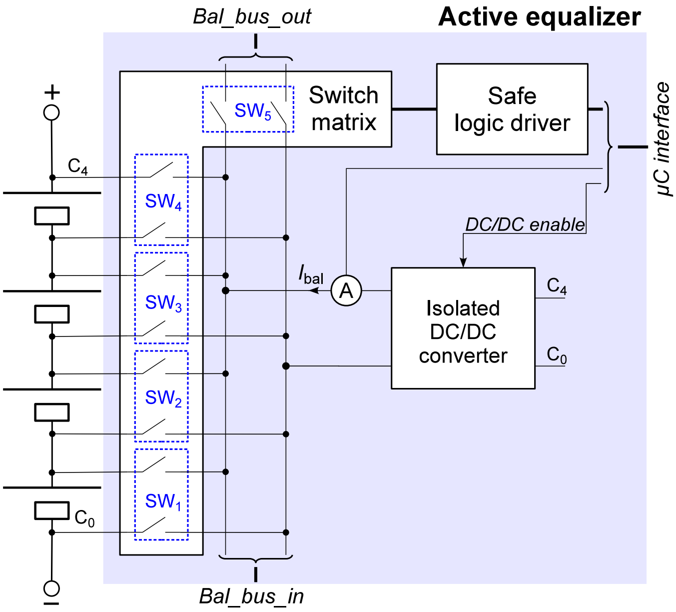

Figure 5. Schematic block diagram of the active charge equalizer.

As stated above, active balancing should allow the battery to deliver all the stored energy to the load. This way, the usable capacity increases from the minimum value to the average one. Such a goal can be achieved by dynamic charge equalization that allows all the cells to reach the discharge cut-off voltage at the same time. This means that the equalizer is used to transfer charge from the cells with higher capacities to those with lower capacity values during the battery discharging. Capacity values can be calculated by accurate estimation algorithms [18], [19]. This attractive approach requires an equalizer circuit capable of delivering high balancing currents. Equation (1) shows the balancing current of the i-th cell (i.e. the charge current that flows into the cell when the terminal battery current is zero) $I_{\mathrm{bal}i}$ needed to obtain a usable capacity equal to C_{u}. I_{pack} is the average discharge battery current and C_i is i-th cell capacity. If the equalizer circuit has a unitary efficiency, the usable capacity can reach the average capacity value.

$$I_{\mathrm{bal}\,i} = \frac{I_{\mathrm{pack}}}{C_{\mathrm{u}}}\left(C_{\mathrm{u}} - C_i\right) \tag{1}$$

One of the main goal of this work is to design an active equalizer circuit that achieves the benefits of dynamic charge equalization. This means that the circuit should deliver a current high enough to perform the required charge redistribution during the battery runtime. Usually, a mobile work machine does not continuously operate between a full charge and a full discharge. Dynamic charge equalization can be applied during the pauses, where recharging might not be available.

Let us now evaluate the performance of dynamic charge equalization when it is applied to the medium-size standard module (i.e. the one with 60 Ah cells), if a 1.5 A balancing current were available. For this purpose, we consider a capacity distribution of the module cells, where one cell capacity is 10 % lower than the nominal value, whereas the other 3 cells have a capacity higher than the nominal one. The average capacity is assumed to be equal to the nominal one. The usable capacity of the module is reduced to 90 % of the nominal value if dynamic charge equalization is not applied. Let us now apply dynamic charge equalization with 1.5 A balancing current. According to (1), all the energy in the module is utilized if the average discharge current I_{pack} is less than 15 A. This value is a quarter of the battery C-rate (a quarter of the nominal cell capacity in ampere), a reasonable value for a mobile work machine. Indeed, it means that the battery has been sized to operate 2 h with a 50 % duty cycle.

Figure 5 shows a schematic view of the active equalizer. The key element to achieve high balancing currents is the very low on-resistance switch matrix, which makes it possible to selectively inject or draw current from each cell of the battery. The isolated DC/DC converter can be designed to transfer energy from the series of the 4 cells to the selected cell, from the selected cell to the series of the 4 cells or in both directions (bidirectional converter). This approach overcomes the limitations in terms of maximum current, volume occupation, and efficiency, which affect the balancing circuit based on transformers with multiple windings or flying capacitors [4]. The design of the switch matrix is derived from that described in [7]. In more detail, each cell terminals can be connected to the inner balancing bus through a solid-state DPST (dual-pole single-throw) switch (SW_1-SW_4). The additional switch SW_5 allows the module balancing to be connected to the balancing bus of the adjacent module to form a closed loop (*Bal_bus_out* of the last module is connected to *Bal_bus_in* of the first module). In this way, energy can be transferred among cells located in different modules (inter-module active balancing).

Each DPST switch consists of a couple of two series-connected MOSFETs (to form a bidirectional switch). The selected MOSFETs (SI7478DP from Vishay) are characterized by a very low on-resistance (7.5 mΩ) and a breakdown voltage of 60 V. The latter value sets the maximum number of standard modules that can share the same balancing bus (which is 4, for the selected MOSFETs). The two couples of parallel-connected gates are driven by the two outputs of the isolated gate driver HT0440 (from Supertex). The two inputs of the HT0440 are driven by the same signal. The five input signals of the switch matrix must be generated in such a way that only and only one DPST switch is on at one time. The violation of this rule leads to catastrophic consequences because it will short-circuit a segment of the battery stack. Thus, the binary-coded selection command of the switch matrix produced by the microcontroller enters the safe logic driver (the design of which is derived from that presented in [7]), which decodes the selection command, and also assures an appropriate deadtime between two different active configurations of the switch matrix.

An off-the-shelf isolated DC/DC converter simplifies the design of the active equalizer. The selected component (EC6A01 from Cincon) provides 7.5 W power on a nominal 5 V output, 9-18 V input range, and 400 V galvanic isolation. As shown in Figure 5, the converter input is the module voltage and the output is connected to the module balancing bus. An Hall effect sensor is employed to measure the output current of the converter. As the active equalizer is a crucial feature of our design, we carried out a preliminary experiment to measure the performance of the DC/DC converter to transfer energy from the 4 series-connected cells of the module to the cell selected through the switch matrix. This measurement was performed connecting a SourceMeter (Keithley 2420) to the converter input to simulate the module voltage and an electronic load (TT*i* LD300) to the converter output to simulate the cell voltage. The achievable balancing current is higher than 1.5 A and the measured efficiency is higher than 70 % in all the voltage range of a $LiFePO_4$ cell (2.5–3.85 V). This proves that the selected DC/DC converter satisfies the design constraints in terms of required balancing current and offers good efficiency.

CONCLUSIONS

The design of a standard battery module consisting of 4 series-connected $LiFePO_4$ cells and the related module management unit has been presented. The concept of the standard module implies that it can be used to assemble the battery for different types of mobile work machines and also to replace a conventional 12 V lead-acid battery largely used in vehicles for starting, lighting and ignition. This creates a wide market for the module with expected important benefits in terms of cost reduction, thus facilitating the growth of electric off-road vehicles. Starting from a hierarchical view of the battery management system, we devised an architecture in which all the functions are concentrated in the module management unit. An innovative feature of the designed unit is the active charge equalizer based on a very low-on resistance switch matrix, a safe logic driver, and an isolated DC/DC converter that provides high balancing current up to 1.5 A. Preliminary experimental tests prove the good efficiency of the charge equalization, which can dynamically be applied during the normal operation of the battery. Current work focuses on the experimental characterization of the module and the development of reliable and accurate state-of-health and state-of-charge algorithms (making the capacity of the cells and the charge stored in them available). This activity will be the basis for the implementation of effective equalization techniques, also based on dynamic charge redistribution among the cells to maximize the usable capacity of the battery.

ACKNOWLEDGMENT

The authors would like to thank Stefano Turchi for his support in designing and manufacturing the MMU boards. This work has been partially supported by the Italian Ministry of Economic Development in the framework of the "Program Agreement: Research on Electric System".

REFERENCES

[1] Y. Gene Liao, M. O'Malley, and A. Quail, "Experimental evaluation of parallel hybrid medium-duty tactical truck," in 2012 IEEE Transportation Electrification Conference and Expo (ITEC), 2012, pp. 1–6.

[2] F. Vellucci, G. Pede, M. Ceraolo, and T. Huria, "Electrification of off-road vehicles : examining the feasibility for the Italian market," in *EVS26 International Battery, Hybrid and Fuel Cell Electric Vehicle Symposium*, 2012, pp. 1–17.

[3] W. C. Lee, D. Drury, and P. Mellor, "Comparison of passive cell balancing and active cell balancing for automotive batteries," in *2011 IEEE Vehicle Power and Propulsion Conference*, 2011, pp. 1–7.

[4] J. Cao, N. Schofield, and A. Emadi, "Battery balancing methods: A comprehensive review," in *Proc. IEEE Vehicle Power and Propulsion Conf. (VPPC)*, 2008, pp. 1–6.

[5] M. Einhorn, W. Guertlschmid, T. Blochberger, R. Kumpusch, R. Permann, F. V. Conte, C. Kral, and J. Fleig, "A Current Equalization Method for Serially Connected Battery Cells Using a Single Power Converter for Each Cell," *IEEE Transactions on Vehicular Technology*, vol. 60, no. 9, pp. 4227–4237, Nov. 2011.

[6] T. A. Stuart and W. Zhu, "Modularized battery management for large lithium ion cells," *Journal of Power Sources*, vol. 196, no. 1, pp. 458–464, 2011.

[7] F. Baronti, G. Fantechi, R. Roncella, and R. Saletti, "High-Efficiency Digitally-Controlled Charge Equalizer for Series-Connected Cells based on Switching Converter and Super-Capacitor," *IEEE Transactions on Industrial Informatics*, vol. 9, no. 2, pp. 1139–1147, 2013.

[8] M. Ceraolo, T. Huria, G. Pede, and F. Vellucci, "Lithium-ion starting-lighting-ignition batteries: Examining the feasibility," in *2011 IEEE Vehicle Power and Propulsion Conference*, 2011, pp. 1–6.

[9] F. Baronti, G. Fantechi, L. Fanucci, R. Roncella, R. Saletti, S. Saponara, and P. Terreni, "Battery Monitoring and Management System per Veicoli Elettrici/Ibridi," in *Progetto H2 Filiera Idrogeno: Risultati e Prospettive*, Pisa: Dedalo, 2012, pp. 55–63.

[10] F. Baronti, G. Fantechi, R. Roncella, R. Saletti, and P. Terreni, "Hardware Building Blocks of a Hierarchical Battery Management System for a Fuel Cell HEV," in *2012 38th Annual Conference on IEEE Industrial Electronics Society (IECON)*, 2012, pp. 1–7.

[11] F. Baronti, G. Fantechi, R. Roncella, and R. Saletti, "Intelligent cell gauge for a hierarchical battery management system," in *2012 IEEE Transportation Electrification Conference and Expo (ITEC)*, 2012, pp. 1–5.

[12] V. R. H. Lorentz, M. M. Wenger, J. L. Grosch, M. Giegerich, M. P. M. Jank, M. Marz, and L. Frey, "Novel cost-efficient contactless distributed monitoring concept for smart battery cells," in *2012 IEEE International Symposium on Industrial Electronics*, 2012, pp. 1342–1347.

[13] Q. Hao, Z. Jianhui, L. Jih-Sheng, W. Yu, and I. T. on Power Electronics, "A High-Efficiency Grid-Tie Battery Energy Storage System," *IEEE Transactions on Power Electronics*, vol. 26, no. 3, pp. 886–896, Mar. 2011.

[14] H. Kim and K. Shin, "{DESA}: Dependable, Efficient, Scalable Architecture for Management of Large-Scale Batteries," *IEEE Transactions on Industrial Informatics*, vol. 8, no. 99, pp. 406–417, May 2011.

[15] M. Zheng, B. Qi, and H. Wu, "A Li-ion battery management system based on CAN-bus for electric vehicle," in *Proc. 3rd IEEE Conf. Industrial Electronics and Applications ICIEA 2008*, 2008, pp. 1180–1184.

[16] H. Rahimi-Eichi, F. Baronti, and M.-Y. Chow, "Modeling and online parameter identification of Li-Polymer battery cells for SOC estimation," in *2012 IEEE International Symposium on Industrial Electronics*, 2012, pp. 1336–1341.

[17] F. Baronti, G. Fantechi, L. Fanucci, E. Leonardi, R. Roncella, R. Saletti, and S. Saponara, "State-of-Charge Estimation Enhancing of Lithium batteries through a Temperature-Dependent Cell Model," in *2011 International Conference on Applied Electronics (AE)*, 2011, pp. 29–33.

[18] M. Einhorn, F. V. Conte, C. Kral, and J. Fleig, "A Method for Online Capacity Estimation of Lithium Ion Battery Cells Using the State of Charge and the Transferred Charge," *IEEE Transactions on Industry Applications*, vol. 48, no. 2, pp. 736–741, Mar. 2012.

[19] M. A. Roscher, J. Assfalg, and O. S. Bohlen, "Detection of Utilizable Capacity Deterioration in Battery Systems," *IEEE Transactions on Vehicular Technology*, vol. 60, no. 1, pp. 98–103, Jan. 2011.